PHYSICAL REVIEW D VOLUME 40, NUMBER 5 1 SEPTEMBER 1989

B-meson decay constant on the lattice and renormalization

Ph. Boucaud, C. L. Lin,* and O. Pène
Laboratoire de Physique Théorique et Hautes Energies, Université de Paris–Sud, F-91405 Orsay, France
(Received 3 February 1989)

We compute in perturbation theory the relation between the B-meson leptonic decay constant F_B computed on a lattice by the $1/m_b$ expansion in the manner of Eichten and the continuum: i.e., the physical value of F_B. To that aim we compare the QCD radiative corrections up to order α_s of the axial-vector-current correlator for different quark masses with the radiative corrections of the effective operator which replaces the correlator in the $1/m_b$ expansion. The latter radiative corrections are computed in the continuum and on a lattice. For this effective operator we recover the anomalous dimension $\gamma=2$ already found by Shifman and Voloshin. Our final result is that $F_B \simeq 0.8 F_B^{\text{latt}}$, only weakly dependent on lattice spacing and Λ_{QCD}.

I. 1/M EXPANSION AND EFFECTIVE OPERATOR

Lattice calculations lead to rather successful estimates of hadron properties: masses, decay constants such as F_π, F_K, etc. When considering states which include one or two charmed quarks the situation becomes trickier since present lattices have $am_c \simeq \frac{1}{2}$ and one has no control on corrections of the order am_c where a is the lattice spacing and m_c the charmed-quark mass. For the b quark the same techniques are out of question since $am_b \gg 1$ for any presently realistic lattice. A new approach is necessary. The basic idea was proposed by Eichten.[1] It consists of performing a $1/m_b$ expansion of the heavy-quark propagator. Then any useful Green's function such as correlation functions can be calculated, to some order in $1/m_b$, only from the knowledge of the light-quark propagator and the gluon fields, which in turn can be estimated on a lattice. In principle with this method one can get an answer from the lattice up to corrections of the order $1/m_b a$ to some power. In fact in what follows we shall stick to the lowest order in $1/m_b a$. Numerical calculations on lattice have already been done[1,2] but they can only give rather loose bounds on F_B by lack of statistics.

We need also to know the exact relation between the lattice result for F_B and its continuum value, and to that aim we must compute the radiative corrections both in the continuum and on the lattice. However, some care is needed since the $1/m_b$ expansion breaks down for the frequencies of gluon fields which are not small compared to m_b.

To state more precisely the problem, let us first recall what happens in the case of F_π (Refs. 3 and 4). One computes the correlation function of two axial-vector currents. These have a vanishing anomalous dimension due to partial conservation of the axial-vector current. The local axial-vector current on the lattice has also no anomalous dimension but it differs from the corresponding operator in the continuum by some finite radiative corrections. These corrections come from the high frequencies which differ on a lattice and in the continuum.

Let us now consider the current $\bar{b}\gamma_\mu\gamma_5 q$. As in the case of F_π the correlation function between two such currents leads to F_B. As we have argued before, the radiative corrections in the continuum are finite (including some logarithmic dependence on m_b). On the lattice the continuum limit would be subtle to find out since it must go in two steps: for $a^{-1} \ll m_b$, one must consider the operator obtained from $1/m_b$ expansion with the b degree of freedom frozen out; but for $a^{-1} \gg m_b$ the b quarks propagate on the lattice and one must compute the original correlation function between $\bar{b}\gamma_\mu\gamma_5 q$ currents. However, this program would be particularly difficult to perform.

Therefore we adopt another strategy. We will use as an intermediate tool the effective operator which results from the $1/m_b$ expansion on the continuum. This operator having an anomalous dimension, its matrix elements depend on the renormalization point. In a first step we compare in the continuum the exact correlation between $\bar{b}\gamma_\mu\gamma_5 q$ currents and the result of the effective operator for a given renormalization point, and in a second step we compare this effective operator on the lattice and in the continuum, for the same renormalization point and for some lattice spacing. Of course, we expect that in the final result any dependence on the continuum renormalization point will disappear.

In the remainder of this section we will summarize the $1/m_b$ expansion, in Sec. II we will compute the relation between the exact current correlator and the effective operator in the continuum, and in Sec. III we will compute the renormalization of the effective operator on the lattice, using Wilson fermions.

A. Formal $1/m_b$ expansion

In the Euclidean metric let us define

$$P(t)=\int d\mathbf{x}\langle(\bar{q}\gamma_0\gamma_5 b)_0(\bar{b}\gamma_0\gamma_5 q)_{\mathbf{x},t}\rangle e^{i\mathbf{p}\cdot\mathbf{x}} . \tag{1.1}$$

At large t the lowest pseudoscalar state dominates the sum over intermediate states:

$$P(t) \underset{t\to\infty}{\sim} \frac{1}{2M_B} |\langle 0|\bar{b}\gamma_0\gamma_5 q|\bar{B}\rangle|^2 e^{-M_B t} = F_B^2 M_B e^{-M_B t} , \tag{1.2}$$

where we have taken $\mathbf{p}=0$. The correlation function in (1.1) can obvioulsy be expressed through a path integral integrated over gauge fields (we assume the quenched approximation):

$$\langle (\bar{q}\gamma_0\gamma_5 b)_0 (\bar{b}\gamma_0\gamma_5 q)_{\mathbf{x},t} \rangle = -\frac{1}{N}\int \mathcal{D}\mathcal{A}\, e^{-S(A)} \times \mathrm{Tr}[S_q(\mathbf{x},t;0)\gamma_0\gamma_5 \times S_b(0;\mathbf{x},t)\gamma_0\gamma_5] , \tag{1.3}$$

where $\mathcal{D}\mathcal{A}$ is the integration measure times the Faddeev-Popov determinant and the gauge-fixing term, S_b (S_q) is the b- (q-) quark propagator in the background gauge field $\mathcal{A}$.

To lowest order in $1/m_b$ the b propagator is equal to[1]

$$S_b(0;\mathbf{x},t) = P\begin{bmatrix} t \\ 0 \end{bmatrix} \delta(\mathbf{x}) \left[\theta(t) e^{-m_b^0 t} \frac{1-\gamma_0}{2} + \theta(-t) e^{m_b^0 t} \frac{1+\gamma_0}{2} \right] , \tag{1.4}$$

where m_b^0 is the lowest-order b-quark mass, i.e., its bare mass, and where

$$P\begin{bmatrix} x_0 \\ y_0 \end{bmatrix} = P \exp\left[ig \int_{y_0}^{x_0} dz_0\, A_{\alpha,0}(0,z_0) t^\alpha \right] \tag{1.5}$$

t^α being the usual color Hermitian matrices. The approximation (1.4) is valid only as long as the background gauge field is smooth enough. If, neglecting for one moment this caveat, we simply substitute (1.4) into (1.3) and (1.1) we get the following approximation for $P(t)$ when $t>0$:

$$P_H(t) = e^{-m_b^0 t} \frac{1}{N} \int \mathcal{D}\mathcal{A}\, e^{-S(A)} \times \mathrm{Tr}\left[\frac{1-\gamma_0}{2} \gamma_0\gamma_5 S_q(0;0,t)\gamma_0\gamma_5 \times P\begin{bmatrix} t \\ 0 \end{bmatrix} \right] . \tag{1.6}$$

Except for the c-number factor $e^{-m_b^0 t}$, the operator whose vacuum expectation value is taken in (1.6) depends only on light quarks and gauge fields. It is a gauge-invariant quantity as expected

On the lattice the Green's function corresponding to (1.6) is

$$P_{\mathrm{latt}}(am_q, m_b, \tau) = e^{-m_b^0 t} \frac{1}{N'} \int d\mu(U) \mathrm{Tr}\left[\frac{1+\gamma_0}{2} S_q^{\mathrm{latt}}(0,\tau;0) \times (U_{1,2} U_{2,3} \cdots U_{\tau-1,\tau}) \right] , \tag{1.7}$$

where $\tau = t/a$. The naive $a \to 0$ limit transforms (1.7) into (1.6) and thus the lattice estimate of (1.7), via Monte Carlo methods, for instance, would give an estimate of (1.1), i.e., of F_B.

B. Radiative corrections and renormalization

We now return to the problem of the high-frequency gluons. They have two effects. First they renormalize the relation between $P_H(t)$ in (1.6) and $P(t)$ in (1.1). Second, as it is well known, the high-frequency gluons are the source of finite differences between the lattice and the continuum, because of the fact that at small distances the discretization of space-time introduced by lattice approximation shows up.

The fact that the radiative corrections introduce differences between (1.1) and (1.6) can be seen through the following argument. The expression (1.1) is the nonlocal product of two partially conserved currents $[\partial_\mu j_\mu^5 = O(m_b)]$ and these currents have (because of Ward identities) a vanishing anomalous dimension. Radiative corrections only bring in finite contributions since for high frequencies (larger than both m_q and m_b) the vertex correction exactly cancels the quark field renormalization diagrams.

On the other hand, the formula (1.6) corresponds to a static b: i.e., an infinite-mass b quark; there is no more current conservation ($\partial_\mu j_\mu^5 \neq 0$), the high-frequency cancellation never occurs, and the sum of all diagrams in Fig. 3 has a logarithmic divergent ultraviolet contribution. It follows, as first noticed in Ref. 5, that the Green's function in (1.6) has a nonvanishing anomalous dimension and its value depends on the renormalization point μ and on the renormalization scheme. The same is true for (1.7) whose value has some $\ln a$ behavior when $a \to 0$ with the same anomalous dimension as (1.6). Our aim is to know the relation between (1.1), which is the physically relevant quantity, and (1.7), which is computable by numerical methods. Being interested in the large-t limit we will define the renormalization constant by

$$P(m_q, m_b, t) \underset{t\to\infty}{\sim} Z(a, m_q, m_b) P_{\mathrm{latt}}\left[am_q, m_b, \frac{t}{a} \right] , \tag{1.8}$$

where we have made explicit the dependence of P (1.1) and P_{latt} (1.7) on the masses.

As we have stated in (1.2) $P(m_q, m_b, t) \sim e^{-M_B t}$ for $t \to \infty$. In this paper we work in perturbation theory in which case the behavior of $P(m_q, m_b, t)$ is dominated for large t by the lightest physical states, i.e., the threshold of the quark-antiquark continuum: it behaves as $e^{-(m_b+m_q)t}$, where m_q and m_b are the "physical masses." By "physical masses" we mean the masses which would be the physical masses in a nonconfining theory, also often called the pole masses, and which have been shown in Refs. 6 and 7 to be renormalization point and renormalization scheme invariant. For the light quark this means that the mass which we take in the right-hand side of (1.8) is not the lattice mass as defined, for example, in Ref. 8 but the pole mass. For the b quark the radiative corrections (see Sec. III) lead to a mass renormalization which diverges in $1/a$ when $a \to 0$. We will fix m_b^0 so that the resulting mass, after radiative corrections, is the pole mass of the b quark.

With these definitions of the masses the threshold is the same on both sides of (1.8), and the ratio between P and P_{latt} is indeed a constant independent of t when $t \to \infty$. In Ref. 2 the bare b mass is also taken with a $1/a$ divergence to compensate the radiative correction, and it is argued that this bare mass is the one which must be used in order to compute $b\bar{b}$ states using static QCD-derived potential from the lattice calculation of the Wilson loops.

In the next two sections we will compute in the Feynman gauge $P(m_q,m_b,t)$ and $P_{\text{latt}}(am_q,m_b,t/a)$. For practical reasons it will be necessary to compute also $P_H(\mu,m_q,m_b,t)$, and we define

$$Z_H(\mu,m_q,m_b)=\lim_{t\to\infty}[P(m_q,m_b,t)/P_H(m_q,m_b,t)] \ . \tag{1.9}$$

II. CONTINUUM RENORMALIZATION

A. Radiative correction to the axial-axial correlator

We want to compute the radiative corrections to $P(m_q,m_b,t)$ defined in (1.1) up to the order α_s. At first sight it seems that we have to compute two-loop diagrams and then a Fourier transform. But if we did the computation this way we would have a hard time dealing with ultraviolet divergences of the quark loop which would play no role in the final result since we need an answer for large t. Typically we assume $t \gg 1/m_q > 1/m_b$. To short circuit this difficulty we will use dispersions relations. To deal with infrared divergences we introduce a gluon mass λ. Of course, no dependence on λ must remain in the final result. Note that the use of gluon mass as an infrared regulator is possible here since we will nowhere use the gluon-gluon coupling in our computation. In order words, our diagrams are QED-like. We start from

$$P(t)=\frac{1}{2\pi}\int dq_0 e^{-iq_0t}\Pi(\mathbf{q}=0,q_0) \ , \tag{2.1}$$

where $\Pi(q)$ is given by the sum of the diagrams schematized in Fig. 1.

For $-q_0^2=s<0$ (Euclidean metric) and from its analyticity $\Pi(s)$ verifies a subtracted dispersion relation:

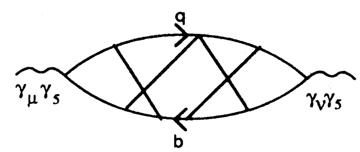

FIG. 1. Schematic representation of the diagrams contributing to $P(t)$.

$$\Pi(s)=\text{polynomial}+\frac{(s-s_1)^n}{2\pi i}\int_{s_0}^{\infty}\frac{2\text{Im}\Pi(s')ds'}{(s'-s)(s'-s_1)^n} \tag{2.2}$$

for any s_1 and for s_0 equal to the physical threshold energy squared. For large t, the polynomial does not contribute. Taking $s_1=0$,

$$P(t)=\frac{1}{(2\pi)^2 i}\int dq_0 e^{-iq_0t}(-1)^n(q_0)^{2n}\int ds'\frac{2\text{Im}\Pi(s')}{(s'+q_0^2)s'^n} \ , \tag{2.3}$$

$$P(t)=\frac{1}{(2\pi)^2 i}(\partial_t)^{2n}\int ds'dq_0 e^{-iqot}\frac{2\text{Im}\Pi(s')}{s'^n(s'+q_0^2)} \ , \tag{2.4}$$

where we have exchanged integrals (both integrals converge). We integrate (2.4) using residues, $q_0=\pm i\sqrt{s'}$, and end up with

$$P(t)=\frac{1}{2\pi}\int_{s_0}^{\infty}\frac{2\text{Im}\Pi(s')}{\sqrt{s'}}e^{-\sqrt{s'}t}ds' \ . \tag{2.5}$$

The main outcome of formula (2.5) is that, for large t, only a small area in the physical cut, just above the threshold, will contribute. In fact when $t \gg 1/m_q, 1/m_b$ one can apply the nonrelativistic approximation to the cut quarks. The cut diagrams that contribute to $\text{Im}\Pi(s')$ are depicted in Fig. 2.

Figure 2(a) leads to (see Appendix A)

$$P^a(t)=e^{-(m_b+m_q)t}\frac{3\sqrt{2}}{\pi^2}\left[\frac{m_bm_q}{t(m_b+m_q)}\right]^{3/2}\Gamma(\tfrac{3}{2}) \ . \tag{2.6}$$

Figures 2(b), 2(c), and 2(d) lead to

$$P^b(t)=P^d(t)=-\tfrac{1}{2}P^c(t)$$
$$=\frac{4\alpha_s}{3\pi}\left[\ln\left[\frac{\lambda t}{2}\right]+\gamma_E+1\right]P^a(t) \ , \tag{2.7}$$

where γ_E is Euler's constant ($\simeq 0.577$).

In the calculation of (2.6) and (2.7) we have assumed $\lambda \ll 1/t \ll m_q, m_b$. From (2.7) the sum of all the diagrams with three cut lines vanishes.

Each of Figs. (2b'), 2(b''), 2(d'), and 2(d'') gives a result proportional to $Z_2^{1/2}-1$, since they only amount to a renormalization of the cut lines (see Appendix A for a discussion of this point) with

$$Z_2(\mu,m,\lambda)-1=-\frac{\alpha_s}{3\pi}\left[\ln\left[\frac{\mu^2}{m^2}\right]+2\ln\left[\frac{\lambda^2}{m^2}\right]+4\right], \tag{2.8}$$

where the mass m is m_b (m_q) for Figs. 2(d′) and 2(d″) [Figs. 2(b′) and 2(b″)], and where we have used the modified minimal subfraction ($\overline{\text{MS}}$) renormalization scheme. Now Figs. 2(c′) and 2(c″) have the same real part and opposite imaginary parts:

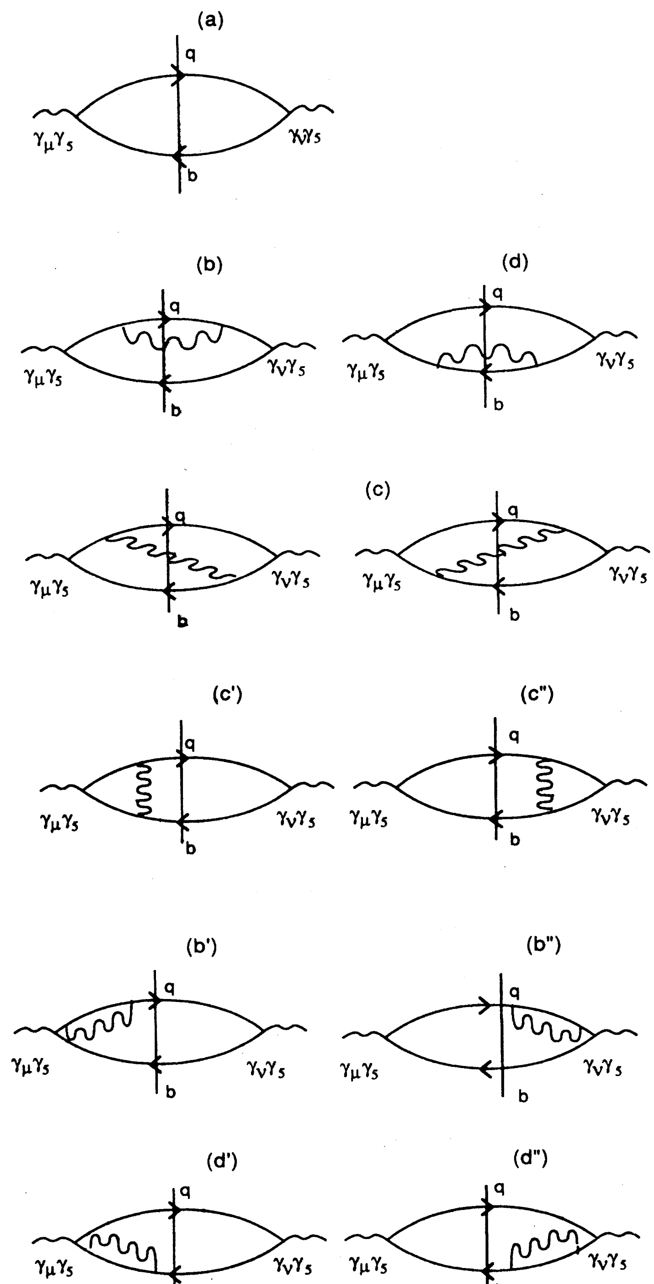

FIG. 2. Cut graphs contributing to the absorptive of $P(t)$.

$$\frac{\mathrm{Re}P^{c'}(t)}{P^a(t)}=+\frac{\alpha_s}{3\pi}\left[\frac{3(m_b-m_q)}{m_b+m_q}\ln\left[\frac{m_b}{m_q}\right]-6\right]+\tfrac{2}{3}\alpha_s\left[\frac{m_b m_q}{m_b+m_q}\right]^{1/2}t^{1/2}\sqrt{2\pi}-[Z_2(\mu,m_b,\lambda)+Z_2(\mu,m_q,\lambda)]\;. \tag{2.9}$$

Finally, the total contribution of diagrams of Fig. 2 leads to

$$P(m_b,m_q,t)=e^{-(m_b+m_q)t}\frac{3\sqrt{2}}{\pi^2}\left[\frac{m_b m_q}{t(m_b+m_q)}\right]^{3/2}\Gamma(\tfrac{3}{2})\times\left\{1+\frac{2\alpha_s}{3\pi}\left[-6+\frac{3(m_b-m_q)}{m_b+m_q}\ln\left[\frac{m_b}{m_q}\right]\right]+\tfrac{4}{3}\alpha_s\sqrt{2\pi}\left[\frac{m_b m_q t}{m_b+m_q}\right]^{1/2}\right\}. \tag{2.10}$$

The self-energy graphs Figs. 2(b′), 2(b″), 2(d′), and 2(d″) lead also to mass renormalizations which do not contribute to the renormalization constant Z (1.8), whence we are not interested here in their exact value. For reasons explained in Sec. I B, we take for the renormalized masses the pole masses and not the ($\overline{\text{MS}}$) ones. It is understood that all the masses in (2.10) are the pole masses, since they give the best estimate of the correlator.[6,7]

B. Renormalization of the effective operator $P_H(t)$

To expand the operator $P_H(t)$ (1.6) up to g^2, we expand both the string operator and the light-quark propagator up to g^2:

$$P\left[\begin{matrix}t\\0\end{matrix}\right]=1+ig\int_0^t A^0(\tau)d\tau-\frac{1}{2}g^2\int_0^t d\tau'\int_0^t d\tau'' A^0(\tau')A^0(\tau'')\;, \tag{2.11}$$

$$S(0,t;0)=S_0(0,t;0)-ig\int d^4x\, S_0(0,t;x)\mathbf{A}(x)S_0(x;0)-g^2\int d^4x\, d^4y\, S_0(0,t;x)\times\mathbf{A}(x)S_0(x;y)\mathbf{A}(y)S_0(y;0)\;, \tag{2.12}$$

where S_0 is the bare propagator, and A^μ are 3×3 Hermitian matrices. Then $P_H(m,t)$ is renormalized by the diagrams depicted in Fig. 3, where the double line depicts the straight temporal line between $(\mathbf{0},t)$ and $(\mathbf{0},0)$, and the gluon propagator coupled to the double line propagates only the time component of the gluon field: $\langle A^0, A^0\rangle$.

Figure 3(a) leads to

$$P_H^a(m,t)=e^{-(m_b+m_q)t}\times\mathrm{Tr}\left[\left[\frac{1-\gamma_0}{2}\right]\gamma_0\gamma_5\left[\frac{1+\gamma_0}{2}\right]\gamma_0\gamma_5\right]\times\frac{3\sqrt{2}}{2\pi^2}\Gamma(\tfrac{3}{2})\left[\frac{m}{t}\right]^{3/2}; \tag{2.13}$$

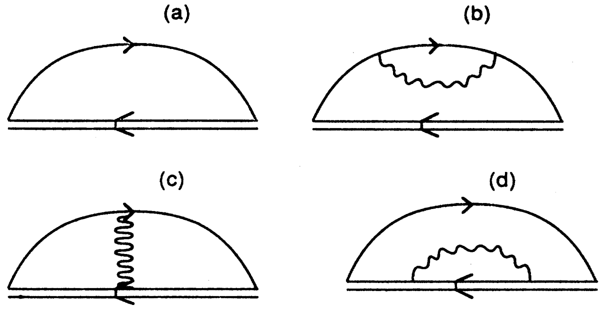

FIG. 3. Graphs contributing to $P_H(t)$ and $P_{\rm latt}(t)$. The double line represents the path-ordered product of gauge fields along a temporal line.

from (2.6) and (2.13) we check that

$$P^a(m_b,m_q,t)=P_H^a(m_r,t)\ , \tag{2.14}$$

where m_r is the reduced mass

$$m_r=\frac{m_b m_q}{m_b+m_q}\underset{m_b\to\infty}{\sim} m_q\ . \tag{2.15}$$

Figure 3(b) gives [cf. Figs. 2(b), 2(b′), and 2(b″)]

$$P_H^b(m,\mu,\lambda,t)=Z_2(\mu,m,\lambda)P_H^a(m,t)+\frac{4}{3}\frac{\alpha_s}{\pi}\left[\ln\left[\frac{\lambda t}{2}\right]+\gamma_E+1\right]P_H^a(m,t) \tag{2.16}$$

with Z_2 in Eq. (2.8).

The graph in Fig. 3(d) is given by

$$P_H^d(m,\mu,\lambda,t)=\frac{-g^2}{2}\frac{4}{3}\mu^{4-d}\times\int_0^t d\tau_1 d\tau_2 G(\tau_2-\tau_1)P_H^a(m,t)\ , \tag{2.17}$$

where d is the dimension (we use $\overline{\rm MS}$ renormalization) and G is the gluon propagator (time component) in the Feynman gauge:

$$G(y)=\int\frac{d^{d-1}k}{(2\pi)^{d-1}}\frac{e^{-\omega|y|}}{2\omega}\ , \tag{2.18}$$

where ω is the gluon energy: $\omega=\sqrt{\mathbf{k}^2+\lambda^2}$. The integral in the right-hand side (RHS) of (2.17) gives

$$I=2\int_0^t dy\,(t-y)\frac{G(y)+G(-y)}{2} \tag{2.19}$$

or

$$I=\frac{2}{(4\pi)^{(d-1)/2}\Gamma\left[\frac{d-1}{2}\right]}\int_0^t dy\,(t-y)\int dk\,k^{d-3}e^{-ky}\ , \tag{2.20}$$

where we have used $\omega=k$ ($\lambda=0$). After some change of variables

$$P_H^d(m,\mu,\lambda,t)=-g^2\frac{4}{3}\frac{(\mu t)^{4-d}}{(4\pi)^{(d-1)/2}\Gamma\left[\frac{d-1}{2}\right]}\times\int_0^1 dx\,(1-x)x^{2-d}\times\int_0^1 dy\,y^{d-3}e^{-y}P_H^a(m,t)\ , \tag{2.21}$$

$$P_H^d(m,\mu,\lambda,t)=-g^2\frac{4}{3}\frac{(\mu t)^{4-d}}{(4\pi)^{(d-1)/2}\Gamma\left[\frac{d-1}{2}\right]}\times\left[\frac{1}{4-d}-\frac{1}{3-d}\right]\Gamma(d-2)P_H^a(m,t) \tag{2.22}$$

we end up with the result

$$P_H^d(m,\mu,\lambda,t)=+\frac{2\alpha_s}{3\pi}\ln\left[\frac{(\mu t)^2e^{2\gamma_E+2}}{4}\right]P_H^a(m,t)\ . \tag{2.23}$$

Note that the coefficient of $\ln\mu$ is different from the one in Z_2, which will lead to a different anomalous dimension for P_H than for P.

We are left with diagram in Fig. 3(c), which is more difficult:

$$P_H^c(m,\mu,\lambda,t)=-\tfrac{4}{3}g^2\mu^{4-d}e^{-m_b t}\int d^4x\int_0^t d\tau\,\mathrm{Tr}\left[\frac{1+\gamma_0}{2}S(t,x)\gamma_0 S(x,0)\right]G(\tau,x_0)\ . \tag{2.24}$$

After Fourier transformation and some manipulations we get

$$P_H^c(m,\mu,\lambda,t)=\tfrac{4}{3}g^2\mu^{4-d}e^{-m_b t}\int\frac{d^dp}{(2\pi)^d}e^{ip_0 t}\mathrm{Tr}\left[\frac{1+\gamma_0}{2}[S_0(p)\gamma_0 J(p)+J(p)\gamma_0 S_0(p)]\right]\ , \tag{2.25}$$

where

$$J(p)=\int\frac{d^dk}{(2\pi)^d}\frac{1}{ik_0}\frac{1}{k^2+\lambda^2}\frac{S(p+k)-S(p-k)}{2}\ . \tag{2.26}$$

After integrating over k and using $\gamma_0=1$ from the projector in (2.25) we get

$$J(p)=-\frac{1}{16\pi^2}\int_0^1 dx\ \ln\left[\frac{\mu^2}{xm^2+x(1-x)p^2+(1-x)\lambda^2}\right]$$
$$-\frac{1}{16\pi^2}\int_0^1\frac{dx}{i}\frac{-i\mathbf{p}\cdot\gamma(1-x)-ip_0+m}{[xp_0^2+x(1-x)\mathbf{p}^2+xm^2]^{1/2}}\ln\left[\frac{[xp_0^2+x(1-x)\mathbf{p}^2+xm^2+(1-x)\lambda^2]^{1/2}+xp_0}{[xp_0^2+x(1-x)\mathbf{p}^2+xm^2+(1-x)\lambda^2]^{1/2}-xp_0}\right]. \quad (2.27)$$

The first term in (2.27) leads to an UV renormalization

$$P_H^{c_1}(m,\mu,\lambda,t)=+\frac{2\alpha_s}{3\pi}\ln\left[\frac{\mu^2e^2}{m^2}\right]P_H^a(m,t) \quad (2.28)$$

up to terms of the order $(1/mt)^{5/2}$. The most subtle part is the evaluation of the second term in (2.27). We refer the reader to Appendix B. We end up with

$$P_H^{c_2}(m,\mu,\lambda,t)=-\frac{4}{3}\frac{\alpha_s}{\pi}\left\{2\left[\ln\left[\frac{\lambda t}{2}\right]+\gamma_E+1\right]-\ln\left[\frac{\lambda^2 t}{m}\right]+\ln(mt)+2-\sqrt{2}\pi^{3/2}\sqrt{mt}\right\}\times P_H^a(m,t)\ . \quad (2.29)$$

From (2.16), (2.23), (2.28), and (2.29) we end up with

$$P_H(m,\mu,t)=\left\{1+\frac{\alpha_s}{\pi}\left[\ln\left[\frac{\mu^2}{m^2}\right]+\frac{4\pi}{3}\sqrt{2\pi}\sqrt{mt}-\tfrac{8}{3}\right]\right\}\times P_H^a(m,t)\ , \quad (2.30)$$

where all dependence on λ has disappeared as expected.

The coefficient of $\ln\mu^2$ in (2.30) agrees with the anomalous dimension $\gamma=2$ found in Refs. 5 and 9 for F_B. From (2.10) and (2.30) we get

$$Z_H(\mu,m_q,m_b)=1-\frac{\alpha_s}{\pi}\ln\left[\frac{e^{4/3}\mu^2}{m_b^2}\right], \quad (2.31)$$

where Z_H has been defined in (1.9)

C. The $m_q\to 0$ limit

The result (2.31) has been achieved under the assumption $\lambda \ll 1/t \ll m_q, m_b$, but we do, of course, believe that it still holds for any value of the ratio $(1/t)/m_q$. Indeed, the difference between $P(t)$ and $P_H(t)$ is of ultraviolet origin and the infrared contributions must cancel exactly. In other words, the difference must have no dependence in the quantities such as $1/t$ or m_q, and we would like to check this independence. Unhappily, it is difficult to check it in the most general way because the analytical formulas become too complicated. We prefer to perform this check in the other extreme limit: $\lambda, m_q \ll 1/t \ll m_b$. This will also help us to be sure that the $\ln m_q$ dependence in (2.10) is a consequence of the approximation $1/t \ll m_q$ and that there remains no mass singularity when $m_q\to 0$. Details of the calculation are given in Appendix D.

We start with the case of P, and we use the same notations as in Sec. II A. From (2.5) and (A2) we get

$$P^a(t)=\frac{3}{\pi^2}\frac{1}{t^3}e^{-m_b t}\ . \quad (2.32)$$

Then we take the $m_q\to 0$ limit of (A10) assuming also that $s-m_b^2 \ll m_b^2$, which corresponds to the assumption $1/t \ll m_b$. A lengthy calculation leads to

$$2k^\mu k^\nu \mathrm{Im}\Pi_{\mu\nu}=\frac{3}{4\pi}y^2\left[1+\frac{g^2}{6\pi^2}(\tfrac{13}{2}+\tfrac{2}{3}\pi^2)+\frac{g^2}{2\pi^2}\ln\frac{m_b^2}{y}\right], \quad (2.33)$$

where $y=s-m_b^2$. As expected, all the singularities in m_q have been canceled. From (2.5) and $y \ll m_b^2$, we get

$$P(t)=\left[1+\frac{\alpha_s}{\pi}\left[\tfrac{4}{3}+2\gamma_E+\tfrac{4}{9}\pi^2+\ln\frac{m_b^2t^2}{4}\right]\right]P^a(t)\ . \quad (2.34)$$

Next we compute the diagrams of Fig. 3 in the case $m=0$. The diagram of Fig. 3(a) leads to

$$P_H^a(t)=\frac{3}{2\pi^2}m_q^3e^{-(m_q+m_b)t}\frac{1}{m_qt}[K_1(m_qt)+K_2(m_qt)]\ \underset{m_q\to 0}{\sim}\ \frac{3}{\pi^2}\frac{1}{t^3}e^{-m_bt}\ . \quad (2.35)$$

Figure 3(b) (massless quark self-energy) leads in $\overline{\mathrm{MS}}$ to

$$P_H^b(t)=-\frac{4}{3}\frac{g^2}{16\pi^2}\ln\left[\frac{\mu^2t^2e^{2\gamma_E}}{4}\right]P_H^a(t)\ . \quad (2.36)$$

The vertex part leads to

$$P_H^c(t)=\frac{4}{3}\frac{g^2}{4\pi^2}\left[\tfrac{1}{2}\ln\left[\frac{\mu^2t^2}{4}\right]+\gamma_E+1+\frac{\pi^2}{3}\right]P_H^a(t)\ . \quad (2.37)$$

Finally, Fig. 3(d) gives obviously the same correction as in the case of nonvanishing m_q (2.23).

Adding (2.23), (2.36), and (2.37) to (2.32) we get

$$P_H(t)=\left\{1+\frac{\alpha_s}{\pi}\left[\ln\left[\frac{\mu^2t^2}{4}\right]+2\gamma_E+\frac{4\pi^2}{9}+\frac{8}{3}\right]\right\}P_H^a(t)\ . \quad (2.38)$$

From (2.38) and (2.34) we get for $Z_H(\mu,m_q,m_b)$ the same result as in (2.31). This is precisely what we expected.

III. LATTICE RENORMALIZATION

We have now to find the connection between the effective correlation functions $P_H(m_q,m_b,t)$ in the continuum (1.6) and $P_{\rm latt}(am_q,m_b,t/a)$ on the lattice (1.7). The relation between the lattice operator

$$O_{\rm latt}(a^{-1})=\bar{q}(0)\frac{1+\gamma_0}{2}U_{0,1}U_{1,2}\cdots U_{t-1,t}q(t) \tag{3.1}$$

and the continuum one in a given renormalization scheme

$$O_{\rm cont}(\mu)=\bar{q}(0)\frac{1+\gamma_0}{2}P \times\left[\exp\left[ig\int_0^t d\tau\, A_{0,\alpha}(\tau,0)\mathbf{t}^\alpha\right]\right]q(t)\ , \tag{3.2}$$

where μ is the renormalization point, can be reasonably computed in perturbation theory if the scales used are much greater than $\Lambda_{\rm QCD}$. Note that the vacuum averages of the operators O in (3.1) and (3.2) differ from the Green's functions defined in (1.6) and (1.7) only by the exponential factor $e^{-m_b^0 t}$ [remember that we do not take the same bare mass in (1.6) and (1.7) in order to compensate the term $\delta^L m_b$ (3.3) and end up with the same pole mass on both sides]. We have

$$O_{\rm cont}(\mu)=Z_{\rm latt}(\mu a,g)O_{\rm latt}(a^{-1})e^{-\delta^L m_b t} \tag{3.3}$$

and $Z_{\rm latt}$ is determined from the $O(g^2)$ corrections to P_H and $P_{\rm latt.}$ We have performed the lattice perturbation theory with the Wilson action for the fermion:

$$S(\psi)=\sum_x\left[-\sum_\mu\frac{1}{2a}[\bar\psi(x)(r-\gamma_\mu)U_\mu(x)\psi(x+\mu)+\bar\psi(x+\mu)(r+\gamma_\mu)U_\mu^+(x)\psi(x)]+\left[m+4\frac{r}{a}\right]\bar\psi(x)\psi(x)\right]\ . \tag{3.4}$$

The $O(g^2)$ corrections to $P_{\rm latt}(t)$ are given by the diagrams of Fig. 3 and are computed by comparison with the corresponding continuum diagrams we have for $P_H(t)$ (see Appendix C).

The large-t behavior of the lattice diagrams is

$$\begin{aligned}
P^a_{\rm latt}(t)&=3\frac{\sqrt{2\pi}}{2\pi^2}m_q^3\left[\frac{1}{m_q t}\right]^{3/2}e^{-m_q t}e^{-m_b^0 t}\ ,\\
P^b_{\rm latt}(t)&=\frac{g^2}{16\pi^2}\frac{4}{3}\left[2\ln(m_q a)+4\ln\left[\frac{m_q t}{2}\right]+5\gamma_E-F_{0000}-\tfrac{1}{2}\right.\\
&\quad\left.+\frac{1}{4\pi^2}\int_{-\pi}^{+\pi}d^4\mathbf{k}\left[\frac{r^2\sum_\lambda\cos k_\lambda}{2\Delta_2}-\frac{\sum_\lambda\sin^2 k_\lambda\sin^2\frac{k_\lambda}{2}}{4\Delta_1^2\Delta_2}+\frac{r^2}{\Delta_2}+\frac{1}{2\Delta_1}\right]\right]P^a_{\rm latt}\ ,\\
P^c_{\rm latt}(t)&=\frac{g^2}{8\pi^2}\frac{4}{3}\left[-2\ln(m_q a)-4\ln\left[\frac{m_q t}{2}\right]-5\gamma_E+F_{0000}-6\right.\\
&\quad\left.+4\pi^2\left[\frac{m_q t}{2\pi}\right]^{1/2}+\frac{1}{4\pi^2}\int_{-\pi}^{+\pi}d^4\mathbf{k}\frac{\sum_\lambda\sin^4\frac{k_\lambda}{2}}{\Delta_1^2\Delta_2}-\frac{1}{4\Delta_2}\right]P^a_{\rm latt}(t)\ ,\\
P^d_{\rm latt}(t)&=\frac{g^2}{16\pi^2}\frac{4}{3}\left[4\ln\left[\frac{t}{2a}\right]+2\gamma_E+F_{0000}+F_{0001}\right]P^a_{\rm latt}(t)e^{-\delta^L m_b t}\ ,
\end{aligned} \tag{3.5}$$

where F_{0000} and F_{0001} are the numerical constants defined in Ref. 10: $F_{0000}\simeq 4.369$ and $F_{0001}\simeq 1.311$; γ_E is the Euler constant;

$$\Delta_1=\sum_\lambda\sin^2\frac{k_\lambda}{2},\quad \Delta_2=\sum_\lambda\sin^2 k_\lambda+4r^2\Delta_1^2\ ,$$

and

$$\delta^L m_b=\frac{4}{3}\frac{g^2}{16\pi^2}\frac{1}{a}\int_{-\pi}^{+\pi}\frac{d^3k}{2\pi^2}\frac{1}{\sum_\lambda(1-\cos k_\lambda)}\ . \tag{3.6}$$

The sum of all diagrams in Fig. 3 amounts to

$$P_{\rm latt}(t)=\left\{1+\frac{\alpha_s}{3\pi}\left[-2\ln(m_q a)-\gamma_E+\frac{2F_{0000}+F_{0001}}{3}-\frac{25}{6}+\frac{1}{12\pi^2}\int_{-\pi}^{+\pi}d^4\mathbf{k}\left[\frac{r^2\sum_\lambda\cos k_\lambda}{2\Delta_2}-\frac{\sum_\lambda\sin^2 k_\lambda\sin^2\frac{k_\lambda}{2}}{4\Delta_1^2\Delta_2}+\frac{2\sum_\lambda\sin^4\frac{k_\lambda}{2}}{\Delta_1^2\Delta_2}+\frac{2r^2-1}{2\Delta_2}+\frac{1}{2\Delta_1}\right]\right]\right\}P^a_{\rm latt}(t)e^{-\delta^L m_b t}\,. \tag{3.7}$$

Comparing (3.7) with (2.30) for $P_H(t)$ we derive the $O(g^2)$ expression for $Z_{\rm latt}$:

$$Z_{\rm latt}=1+\frac{\alpha_s}{\pi}\ln\left[\frac{a^2\mu^2}{C^2}\right], \tag{3.8}$$

where C is defined by

$$\ln C^2=\frac{2F_{0000}+F_{0001}}{3}-\frac{9}{2}-\gamma_E+\frac{1}{12\pi^2}\int_{-\pi}^{+\pi}d^4\mathbf{k}\left[\frac{2\sum_\lambda\sin^4\frac{k_\lambda}{2}}{\Delta_1^2\Delta_2}+\frac{r^2\sum_\lambda\cos k_\lambda}{2\Delta_2}-\frac{\sum_\lambda\sin^2 k_\lambda\sin^2\frac{k_\lambda}{2}}{4\Delta_1^2\Delta_2}+\frac{2r^2-1}{2\Delta_2}+\frac{1}{2\Delta_1}\right]. \tag{3.9}$$

Numerically, $\ln(C^2)\simeq 7.43$ for $r=1$: i.e., $C=41.1$.

It can be useful to know that the contributions to the numerical constant $\ln C^2$ from the different diagrams are 0.17 from Fig. 3(d) (heavy-quark renormalization), 2.97 from Fig. 3(c) (vertex renormalization), 4.29 from Fig. 3(b) (light-quark renormalization).

IV. FINAL RESULT AND CONCLUSION

From formula (2.31) we see that, choosing $\mu^2=m_b^2e^{-4/3}$, we get $P_H(t)=P(t)$. It was expected that this would happen for a value of μ close to m_b since $P_H(t)$ is an approximation of $P(t)$ only for the momentum scales $\ll m_b$. In other terms, we can say that the evolution of (1.1) as a function of the renormalization point has a vanishing anomalous dimension down to the vicinity of m_b and that it gets the anomalous dimension of (1.6) below that region. The coefficient $e^{4/3}$ gives a measure of the effect of the transition between these two regions in the $\overline{\rm MS}$ scheme.

From (3.8) with standard renormalization-group integration we get

$$P_H(\mu,t)=\left[\frac{\alpha_s\left[\frac{C}{a}\right]}{\alpha_s(\mu)}\right]^{4/b}P_{\rm latt}(a,t)\,, \tag{4.1}$$

where a is the lattice spacing, C is the constant defined in (3.9), and $b=\frac{25}{3}$.

We thus end up with

$$P(t)=Z(a,m_q,M_b)P_{\rm latt}(a,t)\,,\qquad Z(a,m_q,M_b)=\left[\frac{\alpha_s(C/a)}{\alpha_s(m_be^{-2/3})}\right]^{12/25}. \tag{4.2}$$

Numerically, we get, for $a^{-1}=2.6\ \mathrm{GeV}^{-1}$, $m_b=4.5$ GeV,

$$Z(a,m_q,M_b)^{1/2}=0.80,\quad \Lambda_{\overline{\rm MS}}=200\ \mathrm{MeV}\,,\qquad Z(a,m_q,M_b)^{1/2}=0.83,\quad \Lambda_{\overline{\rm MS}}=100\ \mathrm{MeV}\,. \tag{4.3}$$

Remember that, from (1.2),

$$F_B=Z^{1/2}F_B^{\rm latt}\,, \tag{4.4}$$

where $F_B^{\rm latt}$ is the result of applying (1.2) with $P_{\rm latt}$ instead of P. In fact $Z(a,m_q,M_b)$ happens to be slowly dependent on a^{-1}, m_b, and $\Lambda_{\overline{\rm MS}}$. For example, keeping $\Lambda_{\overline{\rm MS}}=200$ MeV we get

$$Z(a,m_q,M_b)^{1/2}=0.81,\quad a^{-1}=1.6\ \mathrm{GeV}\,,\qquad Z(a,m_q,M_b)^{1/2}=0.79,\quad a^{-1}=3.0\ \mathrm{GeV}\,. \tag{4.5}$$

The results (4.3) and (4.5) are rather encouraging since they show that the perturbative correction to F_B is only 20%. It raises the hope that the lattice calculations will be able to give a reasonable estimate for F_B when the statistical errors will be sufficiently reduced.

Formula (4.2) also teaches us something about the way the leptonic decay constant F_Q of a $Q\overline{q}$ meson varies (Q being any heavy quark) as a function of the quark mass m_Q and/or the meson mass M_Q. From (1.2) and (4.2) we see that (see also Ref. 5)

$$F_Q^2M_Q\propto[\alpha_s(m_Qe^{-2/3})]^{-12/25}\,, \tag{4.6}$$

which shows that the radiative corrections studied in this paper bring in logarithmic corrections to the zero-order result,

$$F_Q^2M_Q\propto \text{constant independent of } M_Q\,, \tag{4.7}$$

obtained by equating $P(t)$ in (1.2) to $P_H(t)$ in (1.6). The behavior (4.7) is an old result from the quark model: The $Q\bar{q}$ meson wave function becomes independent of m_Q when $m_Q \to \infty$ and this implies (4.7).

The first attempts to compute F_B from the lattice[11,12] have used the formula (4.7) ($F_B^2 M_B = F_D^2 M_D$) and the value of F_D which can be safely computed by the standard method[3,4] as long as $m_c a \ll 1$. The results are $F_B \simeq 85$ MeV (Ref. 11) and $F_B \simeq 74 \pm 12 \pm 21$ MeV (Ref. 12).

However, the use of (4.7) to connect F_B to F_D is questionable, not only because of the absence of the logarithmic corrections in (4.6) but mainly because it is by no means obvious that the charmed quark is heavy enough to allow the use of the asymptotic formulas. Therefore, it has appeared necessary to try a direct Monte Carlo computation of F_B using the technique proposed in Ref. 1 with the more reasonable assumption that the b quark is heavy enough. Unhappily, because of large statistical fluctuations one has up to now only been able to derive an upper bound:[2]

$$F_B \leq 150\,\text{MeV} . \tag{4.8}$$

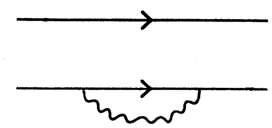

FIG. 4. Quark-propagator renormalization.

In deriving (4.8) the radiative corrections computed in this paper, (4.3) and (4.5), have been used. Obviously more statistics is needed to get a more precise answer.

ACKNOWLEDGMENTS

It is pleasure to thank G. Martinelli, G. Rossi, and J.-P. Leroy for many very useful discussions during all this work. We also thank all the members of the "European Lattice Collaboration" and J. Micheli for fruitful discussions, and M. B. Gavela for a critical reading of the manuscript. Laboratoire de Physique Théorique et Hautes Energies is Laboratoire Associé au CNRS.

APPENDIX A

In this appendix the index 1 (2) refers to the q (b) quark. The diagram of Fig. 2(a) is given by

$$2\,\mathrm{Im}\Pi_{\mu\nu}^{A,a}(k^2) = 3\int \frac{d^4p_1}{(2\pi)^4}\frac{d^4p_2}{(2\pi)^4}(-)\mathrm{Tr}[\gamma_\mu\gamma_5(-\not{p}_2+m_2)\gamma_\nu\gamma_5(\not{p}_1+m_1)]$$
$$\times(2\pi)\delta(p_1^2-m_1^2)(2\pi)\delta(p_2^2-m_2^2)(2\pi)^4\delta_4(k-p_1-p_2)\theta(p_1^0)\theta(p_2^0) \tag{A1}$$

leading to

$$2\,\mathrm{Im}\Pi_{\mu\nu}^{A,a} = (k_\mu k_\nu - k^2 g_{\mu\nu})\frac{2}{4\pi^2}\frac{\pi\omega}{s}\left[1-\frac{m_1^2+6m_1m_2+m_2^2}{2s}-\frac{(m_1^2-m_2^2)^2}{2s^2}\right]$$
$$+k_\mu k_\nu \frac{3}{4\pi^2}\frac{\pi\omega}{s}\frac{(m_1+m_2)^2}{s}\left[1-\frac{(m_1-m_2)^2}{s}\right], \tag{A2}$$

where $s=k^2$ and $\omega=\{\sqrt{[s-(m_1+m_2)^2][s-(m_1-m_2)^2]}\}^{1/2}$. In the k rest frame only the longitudinal part (proportional to $k_\mu k_\nu$) contributes to Π_{00}.

Figure 2(d) gives the longitudinal part

$$2k^\mu k^\nu \mathrm{Im}\Pi_{\mu\nu}^{A,d}(k^2) = \frac{2g^2}{(2\pi)^5}\int d(\mathrm{ps})\frac{1}{(p_2\cdot l)^2}\{8(p_2\cdot l)^2(s+m_1^2+m_2^2)+8(p_1\cdot l)(p_2\cdot l)(m_1^2-m_2^2)$$
$$+(p_2\cdot l)[-8sm_2(m_1+m_2)+16m_2^2(m_2^2-m_1^2)]$$
$$+4m_2^2(m_1+m_2)^2[(m_1-m_2)^2-s]\}, \tag{A3}$$

where d(ps) is the phase space:

$$d(\mathrm{ps}) = d^4p_1 d^4p_2 d^4l\, \delta(p_1^2-m_1^2)\delta(p_2^2-m_2^2)\delta(l^2)\delta_4(k-p_1-p_2-l)\theta(p_1^0)\theta(p_2^0)\theta(l^0) .$$

Figure 2(b) is obtained from (A3) by exchanging p_1 and p_2. Each of Figs. 2(c)–2(c″) gives

$$2k^\mu k^\nu \mathrm{Im}\Pi_{\mu\nu}^{A,c}(k^2) = +\frac{g^2}{(2\pi)^5}\int d(\mathrm{ps})\frac{1}{(p_1\cdot l)(p_2\cdot l)}$$
$$\times\Bigg[16(p_1\cdot l)^2(m_1m_2+m_2^2)+16(p_2\cdot l)^2(m_1m_2+m_1^2)-16(p_1\cdot l)(p_2\cdot l)(s-2m_1m_2)$$
$$-8s(m_1+m_2)[m_1(p_1\cdot l)+m_2(p_2\cdot l)]-8(m_1^2+m_2^2)(m_2^2-m_1^2)(p_1-p_2)\cdot l$$
$$+4s^2(s-m_1^2-m_2^2)\left[\frac{(m_1+m_2)^2}{s}-\frac{(m_1^2-m_2^2)^2}{s^2}\right]\Bigg]. \tag{A4}$$

Adding up Figs. 2(b), 2(c), and 2(d), i.e., the diagrams with three cut lines, and integrating over the phase space we get

$$2k^\mu k^\nu \mathrm{Im}\Pi^{A,(3)}_{\mu\nu}(k^2)=\frac{2g^2\pi^2}{(2\pi)^5}\left\{2(m_1+m_2)^2L_2(s)+4s^2(s-m_1^2-m_2^2)\kappa\left[L_0(s)-\frac{2}{s}\ln\frac{1+v}{1-v}\ln\left[\frac{\lambda}{2(m_1+m_2)}\right]\right]\right.$$
$$-4s^2m_2^2\kappa\left[J_2(s)-\frac{\omega}{sm_2^2}\ln\left[\frac{\lambda}{2(m_1+m_2)}\right]\right]$$
$$\left.-4s^2m_1^2\kappa\left[J_1(s)-\frac{\omega}{sm_1^2}\ln\left[\frac{\lambda}{2(m_1+m_2)}\right]\right]-4s^2\kappa L_1(s)\right\}, \quad \text{(A5)}$$

where

$$\kappa=\frac{(m_1+m_2)^2}{s}-\frac{(m_1^2-m_2^2)^2}{s^2},$$
$$v=\left[\frac{s-(m_1+m_2)^2}{s-(m_1-m_2)^2}\right]^{1/2}$$

and λ is the gluon mass. For the functions J_i, L_i we use the definitions in the Appendix of Ref. 13.

Now we turn to Figs. 2(c′), 2(c″), 2(b′), 2(b″), 2(d′), and 2(d″). Some subtlety arises with the self-energy graphs Figs. 2(b′), 2(b″), 2(d′), and 2(d″). Each self-energy graph has the effect of multiplying the quark propagator by Z_2 so that, naively, we expect these diagrams to multiply the result of Fig. 2(a) by $Z_2^2(\mu,m_q)Z_2^2(\mu,m_b)$. But this is wrong. The point can be made clear if one considers only the propagator of, say, the q quark (Fig. 4). We are looking for the absorptive part of the sum of the two diagrams in

$$S=\frac{1}{p-m+i\epsilon}+\frac{1}{p-m+i\epsilon}\Sigma(p)\frac{1}{p-m+i\epsilon}. \quad \text{(A6)}$$

The result is well known:

$$S=\frac{Z_2}{p-m-\Sigma_R+i\epsilon}, \quad \text{(A7)}$$

where Σ_R vanishes on shell. Now we expect the absorptive part to contain a factor Z_2, not Z_2^2 as naively deduced from Figs. 2(b′) and 2(b″). The problem comes from the fact that a naive estimate of the absorptive part of (A6) has non-well-defined products of distributions of the type $\mathcal{P}(1/z)z\delta(z)$. To get a well-defined result we must keep ϵ finite, compute the imaginary part, and send ϵ to zero at the end of the computations. The result is that

$$\lim_{\epsilon\to 0}\mathrm{Im}\left[\frac{1}{z+i\epsilon}z\frac{1}{z+i\epsilon}\right]=i\pi\delta(z). \quad \text{(A8)}$$

The consequence of (A8) is that the self-energy graphs amount to a factor $Z_2(\mu,m_q)Z_2(\mu,m_b)$ without squares (we thank J.-P. Leroy for this argument). The same result comes out if we apply the cutting rules without self-energy graphs but with renormalized fields in the cut lines. The sum of Figs. 2(c′), 2(c″), 2(b′), 2(b″), 2(d′), and 2(d″), i.e., the diagrams with two cut lines, is given by

$$2k^\mu k^\nu \mathrm{Im}\Pi^{A,(2)}_{\mu\nu}=\frac{3s}{4\pi^2}\pi\omega\frac{g^2\kappa}{6\pi^2}\left\{-\left[3-\frac{3m_1^2+3m_2^2-4m_1m_2}{m_1^2-m_2^2}\ln\frac{m_1}{m_2}-2\left[1-\frac{m_1^2+m_2^2}{m_1^2-m_2^2}\ln\frac{m_1}{m_2}\right]\ln\frac{m_1m_2}{4(m_1+m_2)^2}\right]\right.$$
$$-(m_1-m_2)^2\mathrm{Re}I_0(s)-(m_1-m_2)^2[s-(m_1+m_2)^2]\mathrm{Re}I_1(s)$$
$$+(m_1^2-m_2^2)^2\mathrm{Re}[I_1(s)-I_1(0)]+2s\mathrm{Re}K(s)-2(m_1^2+m_2^2)\mathrm{Re}[K(s)-K(0)]$$
$$-2\left[\left[1-\frac{m_1^2+m_2^2}{m_1^2-m_2^2}\ln\frac{m_1}{m_2}\right]\ln\frac{\lambda^2}{4(m_1+m_2)^2}\right.$$
$$\left.\left.+2s\mathrm{Re}I_0(s)\ln\frac{\lambda}{2(m_1+m_2)}-2s\mathrm{Re}I_1(s)(m_1^2+m_2^2)\ln\frac{\lambda}{2(m_1+m_2)}\right]\right\}. \quad \text{(A9)}$$

Finally the sum of all diagrams in Fig. 2 gives

$$2k^\mu k^\nu \mathrm{Im}\Pi_{\mu\nu} = \frac{3}{4\pi}\omega s\left[\frac{(m_1+m_2)^2}{s} - \frac{(m_1^2-m_2^2)^2}{s^2}\right]$$
$$\times\left[1+\frac{g^2}{6\pi^2}\left\{-\left[3-\frac{3m_1^2+3m_2^2-4m_1m_2}{(m_1^2-m_2^2)}\ln\frac{m_1}{m_2}-2\left[1-\frac{m_2^2+m_2^2}{m_1^2-m_2^2}\ln\frac{m_1}{m_2}\right]\ln\frac{m_1m_2}{4(m_1+m_2)^2}\right]\right.\right.$$
$$-(m_1-m_2)^2\mathrm{Re}\{I_0(s)+[s-(m_1+m_2)^2]I_1(s)\}+(m_1^2-m_2^2)^2\mathrm{Re}[I_1(s)-I_1(0)]$$
$$+2s\mathrm{Re}K(s)-2(m_1^2+m_2^2)\mathrm{Re}[K(s)-K(0)]$$
$$\left.\left.-\frac{2s}{\omega}[m_1^2J_1(s)+m_2^2J_2(s)-(s-m_1^2-m_2^2)L_0(s)+L_1(s)]\right\}\right]+\frac{g^2}{8\pi^3}(m_1+m_2)^2L_2(s) \quad \text{(A10)}$$

in agreement with Eq. (4.2) in Ref. 13, except for the value of $F_A(0)$, for which we agree with Ref. 14. As expected, any dependence in λ has disappeared in (A10) since the sum of the diagrams in Fig. 2 are infrared finite. For the same reason, the $m_2 \to 0$ limit in (A10) must be smooth, and this can indeed be checked (Appendix D).

The correlation function $P(m_2,m_1,t)$ is now given by Eq. (2.5). But the Laplace transform in (2.5) is rather difficult to compute. For the sake of simplicity and since this corresponds to the physical situation (1.2) we want the result in the limit $t \ll 1/m_2, 1/m_1$, equivalent to the limit $|\mathbf{p}| \ll m_2, m_1$. The result is

$$2k^\mu k^\nu \mathrm{Im}\Pi_{\mu\nu}^{NR} = \frac{3\omega}{4\pi}(m_1+m_2)^2\left[1-\frac{(m_1-m_2)^2}{s}\right]\left[1+\frac{2\alpha_s}{3\pi}\left[-6+\frac{3(m_1-m_2)}{m_1+m_2}\ln\frac{m_1}{m_2}\right]+\frac{4}{3}\alpha_s\frac{m_1m_2\pi}{(m_1+m_2)|\mathbf{p}|}\right] \quad \text{(A11)}$$

in agreement with Eq. (A16) in Ref. 15. The Laplace transform (2.5) is now easy to perform, leading to (2.10).

APPENDIX B

We give some details on the calculation of Fig. 3(c). We just consider the first term in (2.27). It contributes to (2.25) for

$$\frac{4}{3}\frac{2}{16\pi}g^2\int_0^1 dx\,\ln\left[\frac{\mu^2}{xm^2+x(1-x)p^2+(1-x)\lambda^2}\right]P_H^{(a)}(m,t)$$
$$=\frac{4}{3}\frac{2}{16\pi^2}g^2\left[\ln\left[\frac{\mu^2e^2}{m^2}\right]+\int_0^1 dx\,\ln\left[\frac{m^2(1-x)}{m^2+xp^2}\right]\right]P_H^{(a)}(m,t)\ . \quad \text{(B1)}$$

The second term in (B1) gives a contribution suppressed by $1/t$ compared to Fig. 3(a). Thus (B1) leads to (2.28). We now consider the second term in (2.27). We define

$$J_2(p) = -\frac{1}{16\pi^2}\int_0^1\frac{dx}{i}\frac{-i(\mathbf{p}\cdot\gamma)(1-x)-ip_0+m}{[xp_0^2+x(1-x)\mathbf{p}^2+xm^2+(1-x)\lambda^2]^{1/2}}\ln\left[\frac{[xp_0^2+x(1-x)\mathbf{p}^2+xm^2+(1-x)\lambda^2]^{1/2}+xp_0}{[xp_0^2+x(1-x)\mathbf{p}^2+xm^2+(1-x)\lambda^2]^{1/2}-xp_0}\right]. \quad \text{(B2)}$$

We have to compute the integral (2.25) with $J(p)$ substituted by $J_2(p)$ (B2). We will first perform the dp^0 integration. To that aim we look for the singularities of $J_2(p)$ and $S_0(p)$ in the upper-half complex p^0 plane. $S_0(p)$ has the well-known poles at $p^0=-i\sqrt{m^2+\mathbf{p}^2}$. The square root in $J_2(p)$ has a branch point at

$$p_0 = i\left[m^2+(1-x)p^2+\frac{1-x}{x}\lambda^2\right]^{1/2}$$

and the cut extends up to $+i\infty$. Let us define $p_0=iy$. For any $y>m$, there is one value of x, x_s such that $\sqrt{-xy^2+x(1-x)p^2+xm^2+(1-x)\lambda^2}$ is real (imaginary) for $x<x_x$ ($x>x_s$).

We also define x_-, x_+, the value of x for which the arguments in the ln of (B2) vanish:

$$-x(1-x)y^2+x(1-x)p^2+xm^2+(1-x)\lambda^2=0\ . \quad \text{(B3)}$$

For $y^2>(m+\lambda)^2+p^2$ the denominator in the ln in (B2) is imaginary with a positive imaginary part if $x_- < x < x_+$. Since $0<x_s<x_-<x_+<1$ we cut the x integral into four parts. For each part we compute the discontinuity in the argument of the integral (B2) for p_0 crossing the cut which is on the positive imaginary axis. The cut in the integrand of (B2) comes out to be

$$\begin{aligned}&0 \quad \text{for } x<x_s\,,\\ &2\pi\frac{-i(p\cdot\gamma)(1-x)+y+m}{\sqrt{xy^2-xm^2-x(1-x)p^2+(1-x)\lambda^2}} \quad \text{for } x_s<x<x_-\,,\\ &0 \quad \text{for } x_-<x<x_+\,,\\ &2\pi\frac{-i(p\cdot\gamma)(1-x)+y+m}{\sqrt{xy^2-xm^2-x(1-x)p^2+(1-x)\lambda^2}} \quad \text{for } x_+<x<1\,.\end{aligned} \tag{B4}$$

The cut contribution to (2.25) is then equal to

$$\frac{4}{3}g^2\frac{1}{16\pi^2}e^{-m_b t}\int\frac{d^3p}{(2\pi)^3}\mathcal{P}\left[\int_m^\infty dy\,e^{-yt}\int_{x_s}^1 dx\frac{4m(y+m)}{y^2-(\mathbf{p}^2+m^2)}\frac{1}{\sqrt{xy^2-xm^2-x(1-x)\mathbf{p}^2-(1-x)\lambda^2}}\right.$$
$$\left.-\int_{\sqrt{(m+\lambda)^2+\mathbf{p}^2}}^\infty dy\,e^{-yt}\int_{x-}^{x+}dx\frac{4m(y+m)}{y^2-(\mathbf{p}^2+m^2)}\frac{1}{\sqrt{xy^2-xm^2-x(1-x)\mathbf{p}^2-(1-x)\lambda^2}}\right], \tag{B5}$$

where we have neglected higher orders in $1/mt$. The second term in (B5) contributes to (2.25) for

$$-\frac{4}{3}\frac{g^2}{2\pi^2}\left[\ln\left[\frac{\lambda t}{2}\right]+\gamma_E+1\right]P_H^{(a)}(m,t) \tag{B6}$$

while the first term in (B5) leads to

$$+\frac{4}{3}\frac{g^2}{4\sqrt{2\pi}}\sqrt{mt}\,P_H^{(a)}(m,t)\,. \tag{B7}$$

In the derivation of (B7) we have used

$$\int_0^B\frac{dx}{1+x}\ln\left[\frac{\sqrt{1+x}+1}{\sqrt{x}}\right]=\ln(B+1)\ln(\sqrt{B+1}+1)+\ln^2(2)-\ln^2(\sqrt{B+1}+1)-\tfrac{1}{4}\ln^2(B+1)$$
$$-2\int_{1/(\sqrt{B+1}+1)}^{1/2}\frac{dx}{x}\ln(1-x)-\frac{1}{2}\int_{1/(B+1)}^{1}\frac{dx}{x}\ln(1-x)\,. \tag{B8}$$

The $B\to\infty$ limit is

$$\int_0^\infty\frac{dx}{1+x}\ln\left[\sqrt{1+x}+\frac{1}{\sqrt{x}}\right]=\frac{\pi^2}{4}\,. \tag{B9}$$

We are left with the contribution of the pole $p^0=i\sqrt{p^2+m^2}$. Let us first consider the case $x<x_s$. It contributes to (2.25) for

$$\frac{g^2}{\pi^2}e^{-mt}e^{-m_b t}\int\frac{p^2dp}{2\pi^2}e^{-(p^2/2m)t}\frac{1}{p}\int_0^1\frac{dx}{\sqrt{1-x^2}}\arctan\left[\frac{m}{p}\frac{x}{\sqrt{1-x^2}}\right] \tag{B10}$$

using, for $m\ll|\mathbf{p}|$,

$$\int_0^1\frac{dx}{\sqrt{1-x^2}}\arctan\left[\frac{p}{m}\frac{x}{\sqrt{1-x^2}}\right]=-\frac{P}{m}\ln\frac{p}{m}+\frac{p}{m} \tag{B11}$$

we find, for the contribution of the pole to (2.25), when $x<x_s$,

$$\frac{4}{3}\frac{g^2}{4\sqrt{2\pi}}\sqrt{mt}-\frac{4}{3}\frac{g^2}{2\pi^2}\left[1+\tfrac{1}{2}\ln mt-\frac{2}{\sqrt{2\pi}}\int p^2dp\,e^{-p^2/2}\ln p\right]P_H^{(a)}(m,t)\,. \tag{B12}$$

For $x>x_s$ the contribution of the pole to (2.25) is

$$\frac{g^2}{2\pi^2}e^{-mt}e^{-m_b t}\int\frac{d^3p}{(2\pi)^3}e^{-(p^2/2m)t}\int_{x_s}^{1}\frac{dx}{\left[x^2\frac{p^2}{m^2}-(1-x)\frac{\lambda^2}{m^2}\right]^{1/2}}\ln\left[\frac{x+\left[x^2\frac{p^2}{m^2}-\frac{(1-x)\lambda^2}{m^2}\right]^{1/2}}{x-\left[x^2\frac{p^2}{m^2}-(1-x)\frac{\lambda^2}{m^2}\right]^{1/2}}\right]; \qquad \text{(B13)}$$

using $x^2(p^2/m^2)-(1-x)\lambda^2/m^2 \ll x$ we get the following contribution to (2.25):

$$\frac{4}{3}\frac{g^2}{4\pi^2}\left[\ln\frac{\lambda^2 t}{m}-\frac{4}{\sqrt{2\pi}}\int_0^\infty p^2dp\, e^{-p^2/2}\ln p\right]P_H^{(a)}(m,t)\,. \qquad \text{(B14)}$$

Now the sum of (B6), (B7), (B12), and (B14) gives (2.29).

One important remark is in order here: adding $P^{c'}(m_b,m_q,\mu,\lambda,t)$ and $P^{c''}(m_b,m_q,\mu,\lambda,t)$ in (2.9) to $P^{c}(m_b,m_q,\mu,\lambda,t)$ in (2.7) and comparing with (2.28) and (2.29) we get

$$p^c(m_b,m_q,\mu,\lambda,t)+P^{c'}(m_b,m_q,\mu,\lambda,t) \underset{m_b\to\infty}{\sim} P_H^{c,1}(m_q,\mu,\lambda,t)+P_H^{c,2}(m_q,\mu,\lambda,t)\,. \qquad \text{(B15)}$$

The result of the vertex graph for the effective operator's Green's function (1.6) P_H is simply given by the $m_b\to\infty$ limit of the vertex graph for the exact Green's function (1.1). Since the same is trivially true for the light-quark self-energy, we conclude that only the heavy-quark self-energy gives different results for the real operators versus the effective operator.

APPENDIX C

In this appendix we give more details on the derivation of (3.5). We need not be too detailed about $P^b_{\rm latt}$ since this is no more than the calculation of $\Sigma_1^{\rm latt}$ already done in literature.[8,16,17] We have checked that we agree with these authors. For example, the agreement of the difference between $P^b_{\rm latt}$ in (3.5) and (2.16) with the difference between Eq. (10b) and (12b) in Ref. 8 is found using the identities

$$F_{0001}-F_{0000}=-\frac{1}{2}-\frac{1}{\pi^2}\int_{-\pi}^{+\pi}d^4k\left[\frac{1}{(4\Delta_1)^2}-\frac{\sum_\mu \sin^2 k_\mu}{(4\Delta_1)^3}\right]$$
$$=-\frac{1}{2}-\frac{1}{4\pi^2}\int_{-\pi}^{+\pi}d^4k\frac{\sum_\mu \sin^4\frac{k_\mu}{2}}{4\Delta_1^3} \qquad \text{(C1)}$$

[see Eq. (3.10) in Ref. 17] and

$$\frac{1}{4}\left[\sum_\mu \sin^2 k_\mu\right]\frac{\sum_\mu \sin^4\frac{k_\mu}{2}-r^2\left[\sum_\mu \sin^2\frac{k_\mu}{2}\right]^2}{\Delta_1^3\Delta_2}$$
$$=\frac{\sum_\mu \sin^4\frac{k_\mu}{2}}{4\Delta_1^3}-\frac{r^2}{\Delta_2}\,. \qquad \text{(C2)}$$

Now we consider $P^c_{\rm latt}(t)$. The equivalent of (2.27) on the lattice is given by

$$e^{m_b^0 t}P^c_{\rm latt}(t)=\sum_{\tau=0}^{t-1}-\tfrac{4}{3}g^2\int_{-\pi}^{+\pi}\frac{d^4p}{(2\pi)^4}e^{ip_0t}\int_{-\pi}^{+\pi}d^4k\,e^{ik_0(\tau+1/2)}\mathrm{Tr}\left[\frac{1+\gamma_0}{2}S(ap)V_0(ap,ap+k)S(ap+k)\right]G_0(k)\,, \qquad \text{(C3)}$$

where τ and t are integers (time expressed in lattice units), S is the quark propagator

$$S(p)=\frac{-i\sum_\mu \gamma_\mu \sin p_\mu + ma + r\sum_\nu(1-\cos p_\nu)}{\sum_\nu \sin^2 p_\nu+\left[ma+r\sum_\nu(1-\cos p_\nu)\right]^2} \qquad \text{(C4)}$$

the vertex $iV_0(p,p+k)$ is given by

$$iV_0(p,p+k)=\left[\gamma_0\cos\left[p_0+\frac{k_0}{2}\right]-i\sin\left[p_0+\frac{k_0}{2}\right]\right] \qquad \text{(C5)}$$

and the gluon propagator is given by

$$G_0(k)=\frac{1}{4\sum_\mu \sin^2\frac{k_\mu}{2}}\,. \qquad \text{(C6)}$$

Let us define

$$J_1(p)=-i\int_{-\pi}^{+\pi}\frac{d^4k}{(2\pi)^4}\frac{e^{ik_0/2}}{e^{ik_0}-1}G_0(k)V_0(p,p+k)\times S(p+k) \qquad \text{(C7)}$$

and

$$J_2(p)=-i\int_{-\pi}^{+\pi}\frac{d^4k}{(2\pi)^4}\frac{e^{ik_0/2}}{e^{ik_0}-1}G_0(k)S(p-k)\times V_0(p-k,p)\,. \qquad \text{(C8)}$$

The lattice equivalent of (2.26) is

$$J(p)=J_1(p)-J_2(p)\ . \tag{C9}$$

Let us call $\bar{J}_1(p)$ and $\bar{J}_2(p)$ the values of (C7) and (C8) with $p=0$ in V_0 and the numerator of S (C4). We get

$$\bar{J}_2(p)-\bar{J}_1(p)=\int_{-\pi}^{+\pi}\frac{d^4k}{(2\pi)^4}\frac{e^{ik_0/2}}{e^{ik_0}-1}\frac{-2i}{4\Delta_1\Delta_2(m)}\left[\cos\frac{k_0}{2}\sin k_0+r^2\sin\frac{k_0}{2}\sum_\lambda(1-\cos k_\lambda)\right], \tag{C10}$$

where

$$\Delta_2(m)=\sum_\mu \sin^2(k_\mu+ap_\mu)+\left[ma+r\sum_\lambda[1-\cos(k_\lambda+ap_\lambda)]\right]. \tag{C11}$$

From (C10), after some manipulation, one obtains

$$\begin{aligned}\bar{J}_2(p)-\bar{J}_1(p)&=-2\int_{-\pi}^{+\pi}\frac{d^4k}{(2\pi)^4}\frac{\cos^2k_0/2+r^2\Delta_1}{4\Delta_1\Delta_2(m)}\\&=-2\int_{-\pi}^{+\pi}\frac{d^4k}{(2\pi)^4}\left[\frac{1}{4\Delta_1\Delta_2}\left[\cos\frac{k_0}{2}-1+r^2\Delta_1\right]+\frac{1}{4\Delta_1\Delta_2(m)}\right],\end{aligned} \tag{C12}$$

where we have replaced $\Delta_2(m)$ by Δ_2 in the term which has a smooth behavior near $k^2=0$.

We then use the identity

$$\int_{-\pi}^{+\pi}\frac{d^4k}{(2\pi)^4}\frac{1}{4\Delta_1\Delta_2(m)}=\frac{1}{16\pi^2}\left[F_{0000}-\gamma_E-\int_0^1 dx\,\ln[(1-x)(xp^2+m^2)a^2]+\frac{1}{4\pi^2}\int_{-\pi}^{+\pi}d^4k\frac{\sum_\mu\sin^4\frac{k_\mu}{2}-r^2\left[\sum_\mu\sin^2\frac{k_\mu}{2}\right]^2}{\Delta_1^2\Delta_2}\right]. \tag{C13}$$

We are left with the difference between $J(p)$ (C9) and (C12). This difference is an ultraviolet finite integral, it depends only on the small-k region, and one can substitute to the lattice integral the continuum one, leading to $P^{c,2}(t)$ as given in (2.29). We end up with the expression of $P^c_{\rm latt}(t)$ given in (3.5)

Now we compute $P^d_{\rm latt}(t)$. The factor which multiplies $P^a_{\rm latt}(t)$ is given by

$$J^d=-\frac{g^2}{2}\frac{4}{3}\sum_{\tau_1,\tau_2=0}^{t-1}G_0(\tau_2-\tau_1) \tag{C14}$$

with

$$G_0(\tau_2-\tau_1)=\int_{-\pi}^{+\pi}d^4k\,e^{ik_0\tau}\frac{1}{4\sum_\mu\sin^2\frac{k_\mu}{2}}\ . \tag{C15}$$

We get

$$J^d=-\frac{4}{3}\frac{g^2}{2}\int_{-\pi}^{+\pi}d^4k\frac{1-\cos k_0t}{1-\cos k_0}\frac{1}{\sum_\lambda(1-\cos k_\lambda)}\ . \tag{C16}$$

Now we use the fact that

$$\frac{1}{1-\cos k_0}=\frac{d}{dk}\left[-\frac{\sin k_0}{1-\cos k_0}\right]$$

and integrate by parts:

$$J^d=-\frac{4}{3}\frac{g^2}{2}\int_{-\pi}^{+\pi}d^4k\,t\left[\frac{\sin k_0}{1-\cos k_0}\frac{\sin k_0t}{2\sum_\lambda(1-\cos k_\lambda)}-2\frac{(1+\cos k_0)(1-\cos k_0t)}{\left[2\sum_\lambda(1-\cos k_\lambda)\right]^2}\right]. \tag{C17}$$

We start with the second term in (C17), which we call $J^{d,2}$. After integration over k we get

$$\begin{aligned}J^{d,2}=\tfrac{4}{3}g^2\int_0^\infty d\alpha\,\alpha e^{-8\alpha}I_0^3(2\alpha)&\\\times\{I_0(2\alpha)+I_1(2\alpha)-I_t(2\alpha)&\\-\tfrac{1}{2}[I_{t+1}(2\alpha)+I_{t-1}(2\alpha)]\}&\ ,\end{aligned} \tag{C18}$$

where I_n are modified Bessel functions (see Ref. 10).

To perform the integration (C18) we split the integral into two parts as done in Eq. (A13) in Ref. 10. We get

$$J^{d,2}=\frac{4}{3}g^2\left\{\frac{1}{16\pi^2}(F_{0000}+F_{0001})-\int_0^1 d\alpha\,\alpha e^{-8\alpha}I_0^3(2\alpha)\left[I_t(2\alpha)+\frac{I_{t+1}(2\alpha)+I_{t-1}(2\alpha)}{2}\right]\right.$$
$$\left.-\int_1^\infty d\alpha\,\alpha\left[e^{-8\alpha}I_0^3(2\alpha)\left[I_t(2\alpha)+\frac{I_{t+1}(2\alpha)+I_{t-1}(2\alpha)}{2}\right]-\frac{2f(t,\alpha)}{(4\pi\alpha)^2}\right]+\frac{1}{8\pi^2}\int_1^\infty d\alpha\frac{1}{\alpha}[1-f(t,\alpha)]\right\}, \tag{C19}$$

where we have chosen $f(t,\alpha)$ according to the asymptotic expansion of I_t:

$$f(t,\alpha)=\frac{\exp\left[\sqrt{t^2+(2\alpha)^2}+t\ln\left[\frac{2\alpha}{t+\sqrt{t^2+(2\alpha)^2}}\right]-2\alpha\right]}{[1+(t/2\alpha)]^{1/4}} \tag{C20}$$

The first integral in (C19) vanishes when $t\to\infty$ as well as the second one, although this takes some pain to prove. We are left with

$$J^{d,2}=\frac{4}{3}g^2\left[\frac{1}{16\pi^2}(F_{0000}+F_{0001})-\frac{1}{4\pi^2}\int_{2/t}^\infty dy\frac{1}{y}\left[e^{-t/2y}-\frac{\exp\left\{t\left[\sqrt{1+y^2}-y+\ln\left[\frac{y}{1+\sqrt{1+y^2}}\right]\right]\right\}}{(1+1/y^2)^{1/4}}\right]\right.$$
$$\left.-\frac{1}{4\pi^2}\int_{2/t}^\infty dy\frac{1}{y}(1-e^{-t/2y})\right]. \tag{C21}$$

One can prove that the first integral in (C21) vanishes in the limit $t\to\infty$ and we end up with

$$J^{d,2}=\frac{4}{3}g^2\left[\frac{1}{16\pi^2}(F_{0000}+F_{0001}+2\gamma_E)+\frac{1}{4\pi^2}\ln\frac{t}{2}\right]. \tag{C22}$$

Let us now consider the first term in (C17). This term is linear in t/a and it contributes to the mass renormalization. Indeed it comes from the terms in (C14) with $\tau_1=\tau_2$ and these would exponentiate in higher orders in g^2. To compute its contribution we note that

$$\frac{\sin k_0 t\,\sin k_0}{2\pi(1-\cos k_0)}$$

converges to the Dirac distribution when $t\to\infty$ (the difference decreases exponentially in t).

Finally we get

$$J^d=\frac{4}{3}g^2\frac{1}{16\pi^2}\left[(F_{0000}+F_{0001}+2\gamma_E)+4\ln\frac{t}{2}\right.$$
$$\left.-\frac{t}{a}\frac{1}{2\pi^2}\int_{-\pi}^{+\pi}d^3k\frac{1}{\sum_\lambda(1-\cos k_\lambda)}\right]. \tag{C23}$$

APPENDIX D

In this appendix we give some details on the calculations in the case of $m_q\to 0$, since they are far from trivial. The most difficult piece concerns formula (2.37). We start from (2.27) with $m=0$. Let us first consider the first term in (2.27). Its contribution to (2.25) has a pole [the $S(p)$ pole] and the cut from ln term. The pole leads to [in the following we omit the multiplicative factor $P_H^a(t)$]

$$\frac{4}{3}\frac{g^2}{8\pi^2}\left[\ln\left[\frac{\mu^2}{\lambda^2}\right]+1\right]. \tag{D1}$$

The cut leads to the factor

$$\frac{4}{3}\frac{g^2}{8\pi^2}\int_0^\infty p^2dp\int_{\lambda t}^\infty e^{-y\sqrt{p^2+1}}(y^2-\lambda^2t^2)$$
$$=\frac{4}{3}\frac{g^2}{4\pi^2}\int_1^\infty\frac{dx}{x}\frac{\sqrt{x^2-1}}{x}(1+x\lambda t)e^{-x\lambda t}$$
$$=\frac{4}{3}\frac{g^2}{4\pi^2}\left[+\gamma_E+\ln\frac{\lambda t}{2}\right]. \tag{D2}$$

Let us now consider the second term in (2.27): i.e., (B2). We first compute the contribution of the numerator to the trace in (2.25):

$$\frac{4}{p_0^2+\mathbf{p}^2}[\mathbf{p}^2(1-x)-p_0^2]. \tag{D3}$$

We thus have to deal with the integral

$$\int_0^{\infty} p^2 \frac{dp}{2\pi^2}\frac{dp_0}{2\pi}\frac{1}{p_0^2+p^2}\int_0^1 \frac{dx}{i}\frac{4[p^2(1-x)-p_0^2]}{[xp_0^2+x(1-x)p^2+(1-x)\lambda^2]^{1/2}}\ln\left[\frac{[xp_0^2+x(1-x)p^2+(1-x)\lambda^2]^{1/2}+xp_0}{[xp_0^2+x(1-x)p^2+(1-x)\lambda^2]^{1/2}-xp^0}\right]. \quad \text{(D4)}$$

The strategy is the same as that in Appendix B. There is a value x_s such that for $x<x_x$ $(x>x_s)$ the pole is out (in) of the cut of the square root. Now $x_+=1$ and the cut contribution to (D4), equivalent to formula (B5), is substituted by

$$\frac{4}{3}g^2\frac{1}{4\pi^2}e^{-m_b t}\int\frac{dp}{(2\pi)^3}\mathcal{P}\left[\int_0^{\infty}dy\, e^{-yt}\int_{x_s}^1 dx\frac{p^2(1-x)+y^2}{y^2-p^2}\frac{1}{\sqrt{xy^2-x(1-x)\mathbf{p}^2-(1-x)\lambda^2}}\right.$$
$$\left.-\int_{\sqrt{\lambda^2+p^2}}^{\infty}dy\, e^{-yt}\int_{x_-}^1 dx\frac{p^2(1-x)+y^2}{y^2-p^2}\frac{1}{\sqrt{xy^2-x(1-x)p^2-(1-x)\lambda^2}}\right], \quad \text{(D5)}$$

where again $p_0=iy$. The first part of (D5) leads, after integrating over x and a change of variables, to

$$\frac{4}{3}g^2\frac{1}{4\pi^2}\mathcal{P}\int_0^{\infty}\frac{dy}{y^3(1-y^2)}\left[\frac{3y^2+1}{2}\ln\left|\frac{y+1}{y-1}\right|-y\right]=\frac{g^2}{6}. \quad \text{(D6)}$$

The cut in the second part of (D5) gives, after a change of variables,

$$-\frac{4}{3}g^2\frac{1}{4\pi^2}\int_0^{\infty}p^2\frac{dp}{2\pi^2}\int_{\sqrt{1+\lambda^2/p^2}}^{\infty}dy\frac{e^{-pyt}}{1-y^2}\left[\frac{3y^2+1-\frac{\lambda^2}{p^2}}{2}\ln\left[\frac{(y+1)^2-\frac{\lambda^2}{p^2}}{y^2-1-\frac{\lambda^2}{p^2}+\frac{2p\lambda^2}{p^2(y-p)}}\right]-y+\frac{\lambda^2 y}{(y^2-1)p^2}\right]. \quad \text{(D7)}$$

To deal with the infrared singularity near the lower bound of y we cut the integral into two parts below/above $\sqrt{1+\delta^2}$ with $\lambda^2/p^2 \ll \delta^2 \ll 1$. After some work we end up with the result (once P_H^a has been factorized out)

$$-\frac{g^2}{6\pi^2}\int_0^{\infty}p^2dp\left[-\ln^2\frac{2p}{\lambda t}+\ln\frac{2p}{\lambda t}+\frac{\pi^2}{4}-1\right]. \quad \text{(D8)}$$

The pole term in (D4) for $x<x_s$ [equivalent to (B10) and (B12)] gives

$$\frac{g^2}{3\pi^2}\int_0^{\infty}p^2\frac{dp}{2}e^{-pt}\int_0^{x_s}dx\frac{p(2-x)}{\sqrt{(1-x)\lambda^2-x^2p^2}}\arctan\left[\frac{xp}{\sqrt{(1-x)\lambda^2-x^2p^2}}\right]=\frac{g^2}{12} \quad \text{(D9)}$$

and the pole term for $x_s<x$ [equivalent to (B13) and (B14)] gives

$$\frac{g^2}{3\pi^2}\int_0^{\infty}p^2\frac{dp}{2}e^{-pt}\int_{x_s}^1 dx\frac{p\left[1-\frac{x}{2}\right]}{\sqrt{(1-x)\lambda^2-x^2p^2}}\ln\left[\frac{xp+\sqrt{(1-x)\lambda^2-x^2p^2}}{xp-\sqrt{(1-x)\lambda^2-x^2p^2}}\right]=-\frac{g^2}{6\pi^2}\int_0^{\infty}p^2dp\left[\ln^2\frac{2p}{\lambda t}-\ln\frac{2p}{\lambda t}+\frac{\pi^2}{6}+\frac{1}{2}\right]. \quad \text{(D10)}$$

Adding (D1), (D2), (D6), and (D8)–(D10) leads to (2.37).

We now add a few words about the computation of the light-quark self-energy diagram (2.36) in the massless limit:

$$\Sigma(p)=\int_0^1 dx\, 2(1-x)i\not{p}\ln\left[\frac{\mu^2 e}{(1-x)(xp^2+\lambda^2)}\right]. \quad \text{(D11)}$$

Figure 2(b) gives then

$$\frac{g^2}{12\pi^2}2ie^{-m_b t}\int_0^{\infty}p^2\frac{dp}{2\pi^2}\frac{dp_0}{2\pi}e^{ip_0 t}\frac{p_0}{p_0^2+p^2}\left[\ln\left[\frac{\mu^2 e}{p_0^2+p^2+\lambda^2}\right]\right.$$
$$\left.-2\frac{\lambda^2}{p_0^2+p^2}\ln\left[\frac{p_0^2+p^2+\lambda^2}{\lambda^2}\right]+\frac{\lambda^2}{p_0^2+p^2}-\left[\frac{\lambda^2}{p_0^2+p^2}\right]\ln\left[\frac{p_0^2+p^2+\lambda^2}{\lambda^2}\right]\right]. \quad \text{(D12)}$$

The contribution from the poles in (D12), having now factorized out $P_H^a(t)$, is equal to

$$-\frac{g^2}{12\pi^2}\left[\ln\left[\frac{\mu^2 e}{\lambda^2}\right]-\frac{3}{2}\right]. \quad \text{(D13)}$$

The contribution of the cut to (D12) is

$$-\frac{g^2}{12\pi^2}\left[\tfrac{1}{2}+2\gamma_E+\ln\frac{\lambda^2t^2}{4}\right]. \tag{D14}$$

The sum of (D13) and (D14) leads to (2.36).

---

*Permanent address: Soochow University, Taipei, Taiwan, Republic of China.

[1]E. Eichten, in *Field Theory on the Lattice,* proceedings of the International Symposium, Seillac, France, 1987, edited by A. Billiore *et al.* [Nucl. Phys. B (Proc. Suppl.) **4**, 140 (1988)]; see also E. Eichten and F. Feinberg, Phys. Rev. D **23**, 2724 (1981).

[2]Ph. Boucaud, O. Pène, V. Hill, C. T. Sachrajda, and G. Martinelli, Phys. Lett. B **220**, 219 (1989).

[3]G. Martinelli and Y. C. Zhang, Phys. Lett. **123B**, 433 (1983); **125B**, 77 (1983).

[4]M. Bochicchio, L. Maiani, G. Martinelli, G. Rossi, and M. Testa, Nucl. Phys. **B262**, 331 (1985).

[5]M. A. Shifman and M. B. Voloshin, Yad. Fiz. **45**, 463 (1987) [Sov. J. Nucl. Phys. **45**, 292 (1987)].

[6]S. Narison, Phys. Lett. B **197**, 405 (1987).

[7]R. Tarrach, Nucl. Phys. **B183**, 384 (1981).

[8]A. Gonzales Arroyo, F. J. Yndurain, and G. Martinelli, Phys. Lett. **117B**, 437 (1982).

[9]H. D. Politzer and M. B. Wise, Phys. Lett. B **206**, 681 (1988).

[10]A. Gonzales Arroyo and C. P. Korthals Altes, Nucl. Phys. **B205**, 46 (1982).

[11]M. B. Gavela, L. Maiani, S. Petrarca, G. Martinelli, and O. Pène, Phys. Lett. B **206**, 113 (1988).

[12]C. Bernard, T. Draper, G. Hockney, and A. Soni, Phys. Rev. D **38**, 3540 (1988).

[13]K. Schilcher, M. D. Tran, and N. F. Nasrallah, Nucl. Phys. **B181**, 91 (1981).

[14]M. B. Gavela, A. Le Yaouanc, L. Oliver, O. Pène, and J.-C. Raynal, Phys. Rev. D **22**, 2906 (1980).

[15]J. E. Paschalis and G. J. Gounaris, Nucl. Phys. **B222**, 473 (1983).

[16]W. Hamber and C. M. Wu, Phys. Lett. **133B**, 351 (1983).

[17]C. Bernard, A. Soni, and T. Draper, Phys. Rev. D **36**, 3224 (1987).